Phosphorylation of eIF4GII and 4E-BP1 in response to nocodazole treatment: a reappraisal of translation initiation during mitosis

Article (Accepted Version)

Phosphorylation of eIF4GII and 4E-BP1 in response to nocodazole treatment – a reappraisal of translation initiation during mitosis.

Mark J. Coldwell[a*], Joanne L. Cowan[a*], Markete Vlasak[b], Abbie Mead[a], Mark Willett[b], Lisa S. Perry[a], and Simon J. Morley[b]

[a]Centre for Biological Sciences, University of Southampton, Southampton, SO17 1BJ, UK; [b]School of Life Sciences, University of Sussex, Falmer, Brighton BN1 9QG, UK; *These authors contributed equally to the manuscript.

Corresponding authors

Mark J. Coldwell, Centre for Biological Sciences, University of Southampton, Southampton SO17 1BJ, UK

Tel: 023 80594342

e-mail: M.Coldwell@soton.ac.uk

Simon J. Morley, School of Life Sciences, University of Sussex, Falmer, Brighton BN1 9QG, UK

Tel: 01273 678510

e-mail: S.J.Morley@sussex.ac.uk

Short title Translation initiation factor modifications during mitosis

Keywords Eukaryotic translation initiation factor, cell cycle, nocodazole, Cdk1, eIF4GII, 4E-BP1

Abbreviations

4E-BP, eIF4E-binding protein; CAMK1, Calcium/calmodulin-dependent protein kinase type 1; Cdk1, cyclin-dependent kinase 1; eIF, eukaryotic initiation factor; FACS, fluorescent-activated cell sorting; IRES, internal ribosome entry site; mTORC1, mammalian target of rapamycin complex 1; PABP, poly(A)-binding protein; PKC, Protein kinase C.

Abstract

Translation mechanisms at different stages of the cell cycle have been studied for many years, resulting in the dogma that translation rates are slowed during mitosis, with cap-independent translation mechanisms favoured to give expression of key regulatory proteins. However, such cell culture studies involve synchronisation using harsh methods, which may in themselves stress cells and affect protein synthesis rates. One such commonly used chemical is the microtubule de-polymerisation agent, nocodazole, which arrests cells in mitosis, and has been used to demonstrate that translation rates are strongly reduced (down to 30% of that of asynchronous cells). Using synchronised HeLa cells released from a double thymidine block (G_1/S boundary), or the Cdk1 inhibitor, RO3306 (G_2/M boundary), we have systematically re-addressed this dogma. Using FACS analysis and pulse-labelling of proteins with labelled methionine we now show that translation rates do not slow as cells enter mitosis. This study is complemented by studies employing confocal microscopy which show enrichment of translation initiation factors at the microtubule organising centres, mitotic spindle and midbody structure during the final steps of cytokinesis, suggesting that translation is maintained during mitosis. Furthermore, we show that inhibition of translation in response to extended times of exposure to nocodazole reflects increased eIF2α phosphorylation, disaggregation of polysomes, and hyperphosphorylation of selected initiation factors, including novel Cdk1-dependent N-terminal phosphorylation of eIF4GII. Our work suggests that effects on translation in nocodazole arrested cells might be related to those of the treatment used to synchronise cells rather than cell cycle status.

Introduction

Protein synthesis is carried out in three stages (initiation, elongation and termination), with the initiation stage of translation generally accepted as a major site of regulation of gene expression.[1-6] This pivotal role reflects the regulated binding of mRNA to the ribosome, facilitated by the assembly of eIFs (eukaryotic initiation factors) into a multi-protein complex known as eIF4F (composed of eIF4E, eIF4A and eIF4G) which associate with the 7-methylguanylate (m^7G) cap structure at the 5' end of the mRNA. eIF4G is expressed as two paralogues in mammalian cells, eIF4GI and eIF4GII. Although initial reports suggested eIF4GI and eIF4GII were interchangeable,[7] over-expression of the eIF4GII paralogue in an eIF4GI knockdown background was unable to restore translation to the same extent as eIF4GI.[8]

In turn, the activity of the eIF4F complex is regulated by both phosphorylation and the inherent structural properties of the recruited mRNA.[1, 4, 6] The formation of the eIF4F complex reflects the regulated availability of eIF4E to participate in initiation, a process controlled by a number of general and mRNA-specific regulatory proteins. Using a conserved motif, 4E-BPs (eIF4E-binding proteins) compete with the eIF4Gs for a common surface on eIF4E and inhibit eIF4F assembly. The regulated association of 4E-BPs with eIF4E is acutely modulated by multi-site phosphorylation dependent upon mammalian target of rapamycin complex 1 (mTORC1) signalling,[2, 5] effectively integrating signals from mitogens and nutrients with the translational apparatus.[2, 3] In addition to modification of the eIF4 family of proteins, phosphorylation of the α-subunit of the canonical initiation factor eIF-2 has been shown to be increased at G_2/M.[9] This phosphorylation has been shown to have a permissive effect on the efficiency of cap-independent initiation of translation at two cell cycle-dependent internal ribosome entry sites (IRESs), thereby mediating specific mRNA translation at this phase of the cell cycle.[9]

Work over a number of years has suggested that the rate of protein synthesis varies throughout the cell cycle.[10-12] In HeLa cells arrested in mitosis using colcemid, cap-dependent, but not IRES-mediated, translation initiation was impaired along with a dephosphorylation of eIF4E.[13] In nocodazole-arrested HeLa cells, 4E-BP1 was shown to be in a more hypophosphorylated state, interacting strongly with eIF4E, decreasing eIF4F complex levels.[11] The same study showed that eIF4GII was hyperphosphorylated during nocodazole treatment of cells which correlated with a decrease in its binding to eIF4E. In contrast, in HeLa cells synchronised and released from a sequential thymidine and aphidicolin block, phosphorylation of 4E-BP1 was increased at Thr-70 by the cyclin-dependent kinase, Cdk1, with phosphorylation of this site being permissive for Ser-65 phosphorylation.[14]

Using synchronised HeLa cells incubated with nocodazole, the Cdk1 inhibitor, RO3306, or released from a double thymidine block, we have systematically re-addressed whether rates of protein synthesis are changed during mitosis and how this correlates with initiation factor phosphorylation. The work described here indicates that exposure of cells to nocodazole promotes increased eIF2α phosphorylation and disaggregation of polysomes, characteristics of an inhibition of initiation. However, this was not observed with cells released from a G_1/S block using the double-thymidine approach. Furthermore, we have teased apart some of the phosphorylation events that occur in response to nocodazole, and present here a reappraisal of how initiation factor complexes are effected in response to this treatment.

Results

Translation rates are maintained throughout the cell cycle, and initiation factors are associated with components of the tubulin cytoskeleton during mitosis

Double thymidine block was used to synchronise exponentially growing HeLa cells at the G_1/S phase border. Cells were then released from this block and the nuclear content analysed by propidium staining and flow cytometry analysis showing that a cycle was completed within 20 hours (Figure 1A). The majority of mitosis was observed to occur between 8 and 11 hours post-release. These results are in agreement with previous work.[15] In parallel experiments, the incorporation of [^{35}S] Methionine into precipitable protein was measured for the 30 minutes prior to harvest in order to gauge whether there was a decrease in protein synthesis rate in cells going through M phase. While translation rates did fluctuate during the cell cycle, there was no decrease observed at any of the time points where the majority of cells were undergoing mitosis (Figure 1B). In comparison, in cells that were synchronised with thymidine, released then incubated with nocodazole, there was a robust decrease in translation to around ~30% of that of asynchronous cells, in agreement with previous work.[16]

Immunoblotting of cell extracts showed that the levels of the cell cycle markers Cyclin B1 and Survivin increased and decreased as predicted throughout the timecourse (Figure 1C). When determining the influence of the cell cycle stages on members of the translation initiation factor machinery, there were no changes in levels of components of the eIF4F complex (eIF4GI, eIF4A and eIF4E) and no increased phosphorylation of eIF2α was observed. There was an upward shift in mobility of 4E-BP1 in cells in early G_1 and immediately post M phase (12-14 hours post release), suggesting an increase in phosphorylation. According to models of translational control, these results all point to a generally favourable environment for translation to proceed.

The results from Figures 1B and C indicate that, rather than there being a reduction in protein synthesis associated with passage into mitosis, translation is maintained at a relatively consistent level throughout the cell cycle. We and others have previously shown that a subpopulation of components of the initiation factor machinery are localised to the nucleus.[17] We therefore embarked on confocal microscopy experiments to examine how these proteins localise in cells in which the nuclear membrane undergoes breakdown,[18] thus removing the physical barrier between the cytoplasm and nucleoplasm. We examined synchronised cells that were proceeding through mitosis (Figure 2), staining cells for a component of the translation machinery (eIF4GI, PABP, eIF4E, 4E-BP1 or ribosomal protein S6) alongside α-tubulin and DNA, the definitive morphologies of which could be used to define the various characteristic stages. At each stage co-localisation of each component was observed with the tubulin cytoskeleton, implying that there may be some ongoing translation localised to this important component of the cell. This perhaps aids in the synthesis of further tubulin, or other components (e.g. chromosomal passenger proteins) which are required for efficient mitosis.

Synchronisation in M phase with nocodazole inhibits translation rates and leads to robust phosphorylation of key translation factors

Given that our work showed that there was unlikely to be any inhibition of translation in cells transiting through mitosis, we returned to those which had undergone treatment with nocodazole,

to determine the underlying mechanisms of the observed reduction in protein synthesis (Figure 1B). FACS analysis showed the expected peak of cells arrested in G_2/M when compared to cells maintained in an asynchronous state (Figure 3A), and sucrose density gradients show that nocodazole treatment leads to a reduction in polysomes, a further confirmation of the inhibition of protein synthesis (Figure 3B). Extracts from asynchronous cells or those having undergone thymidine/nocodazole synchronisation showed that there was a strong phosphorylation of the alpha subunit of eIF2 on Ser 51 (Figure 3C), confirming the work of others.[16] This post-translational modification inhibits the eIF2B guanine nucleotide exchange factor, which prevents the recycling of eIF2 from a GDP to a GTP bound state, thus preventing ternary complex formation (eIF2·Met-tRNAi·GTP), thus inhibiting further rounds of translation initiation. Other modifications of translation initiation factors were observed, with a retarded migration observed of eIF4GI, eIF4GII and of some of the 4E-BP1 population (Figure 3C). The maintenance of a proportion of 4E-BP1 in a hypophosphorylated (termed "α") state shows another situation which would be likely to inhibit translation. This phosphor-form of the protein is able to bind to and sequester eIF4E and inhibit the interaction of this cap-binding protein with the eIF4G proteins, which act as molecular "scaffolds" onto which a number of other factors bind. However, we also observed that around 70% of the 4E-BP1 migrated higher than the standard phosphor-forms of the proteins, reflecting modification over and above those already established. This modification was not prevented by preincubation of cells with the mTOR inhibitor RAD001 (Figure S1). We used our low percentage SDS-PAGE method[19] to enable delineation of eIF4G isoforms which arise through alternative translation initiation from either different AUGs (in the case of eIF4GI[20, 21]) or a CUG and AUG (eIF4GII[8]) and therefore differ at their N-termini. The shift in migration was observed in all the isoforms, (Figure 3C) suggesting that no one eIF4G isoform is subjected to differential regulation. Both these factors, and 4E-BP1 are known phosphoproteins, so we next analysed whether the migratory changes were due to phosphorylation.

Extracts from asynchronous or nocodazole treated cells were prepared, and then treated with bacteriophage lambda protein phosphatase (Figure 3D). In all cases, the nocodazole-dependent changes in migration or phosphorylation were either greatly reduced or completely abrogated, suggesting that phosphorylation is the post-translational modification underlying these observations. In the case of eIF4GII, it was also observed that there is an underlying phosphorylation in asynchronously maintained cells, which is likely to be due to phosphorylation at alternative sites to those modified in this treatment.[22]

Robust phosphorylation of eIF2α and 4E-BP1 does not occur following release from G_2/M block or with reduced incubation with nocodazole

To investigate the nocodazole-dependent phosphorylation of initiation factors in more detail, we employed an alternative mechanism to arrest cells at the G_2/M border. Phosphorylation of key substrates by the Cdk1/cyclin B complex acts as a trigger for the commitment to mitosis, and so the reversible cell-permeable small molecule Cdk1 inhibitor RO3306[23] was employed, as it acts in an independent manner to those like nocodazole which act on microtubule dynamics. In our experience, we have struggled to release cells from the nodazole-induced arrest, but this is issue is not the case when using RO3306. Therefore, following removal of this inhibitor from the cell medium, the cell cycle status was assayed by FACS in comparison to asynchronous cells, or those arrested by thymidine nocodazole block (Figure 4A), and translation rates measured as before (Figure 4B), albeit

with a shorter 15 minute pulse of [^{35}S] methionine prior to harvest. While we did observe some inhibition of protein synthesis in the cells treated with RO3306, this was not as strong as that observed with nocodazole and we measured no further reduction in translation rates as cells progressed through mitosis. Analysis of extracts prepared from these cells (Figure 4C) showed that there was no shift in migration of eIF4GI, only a slight phosphorylation of eIF2α and a transient limited migration of 4E-BP1 to the upper forms. This suggests that any of the changes of signalling events to these proteins are only limited or transitory, but exposure to nocodazole itself maybe creating a situation where the modifications are maintained for too long, thus allowing a state of reduced translation to develop.

To further determine the effects of sustained incubation with nocodazole, we again synchronised cells by double thymidine block, and then post-release incubated them without nocodazole or by adding nocodazole at different times. This would induce the arrest as usual, but the nocodazole would only have been present for less time than in the standard protocol. FACS analysis showed that the nocodazole induced the expected arrest, whether added at an initial or later time after release of the thymidine block (Figure 4D). Pulse labelling of cells with [^{35}S] methionine prior to harvest showed that there was only a limited inhibition of protein synthesis at the last time point (Figure 4E), by which point some of the cells which would have otherwise completed mitosis would have been arrested for around 4 hours, rather than the 20 hours utilised in the standard protocol. It is therefore not surprising that the modifications of eIF2α and 4E-BP1 were also only observed at later timepoints in these cells, and at a limited level as determined by immunoblotting (Figure 4F).

In addition to the four mTORC1-dependent phosphorylation sites of 4E-BP1 identified at Thr 37, Thr 46, Ser 65 and Thr 70,[24, 25] other phosphorylation sites were postulated at Ser 83 and Ser 112.[26, 27] Therefore, we attempted to identify if these were the sites modified following nocodazole treatment. A cDNA corresponding to the open reading frame of 4E-BP1 was obtained by RT-PCR of HEK293 cell RNA and subcloned into a vector which fused a myc-tag to the N-terminus and 3 copies of the FLAG tag to the C-terminus. This vector was then subjected to site-directed mutagenesis to convert the serines at 83 and 112 to alanines, either singly or together. The wild-type vector and the three mutated variants were then transfected into HeLa cells which were incubated with or without nocodazole (Figure 4G). Although it is not as obvious as observed with the endogenous protein (possibly due to the overexpression of the exogenous tagged 4E-BP1) there is an upward shift in response to nocodazole with the WT and S112A variants. However, the movement of S83A is less evident, perhaps indicating that this residue is a further site of phosphorylation in cells treated with nocodazole. Previous work has shown that 4E-BP1 can be phosphorylated by Cdk1 in vitro[14] and it is possible that a further threonine residue could be a subsequent target following phosphorylation at Thr 70 by this kinase. Given these results, Thr 82 could perhaps be such a site. To this end we created further mutants (T82A and T82A/S83A) to examine if the nocodazole dependent modifications were abrogated. To aid in the identification of the phosphoforms of both endogenous and exogenous proteins, the membrane was probed with both murine anti-FLAG and leporine anti-4E-BP1, which enabled us to visualise the migration using appropriate species-specific fluorescently tagged secondary antibodies. Our results (Figure 4H, upper panel) show that Thr 82 is not likely to be a phosphosite as the upward shift is still observed in T82A (compare lanes 4 and 6). However, the relative lack of a shift in the T82A/S83A mutant does again confirm that while Ser 83 may be the residue modified in the presence of nocodazole, or be modified in tandem with Thr 82, but neither of these is the major site of phosphorylation. The large shift observed in the endogenous 4E-BP1

could indicate that nocodazole treatment affects a pair of phosphosites, and it is a consequence of overexpressing exogenous 4E-BP1 that prevents us observing these modifications to their full extent. Indeed, probing the membrane with an anti-4E-BP1 antibody shows the substantial expression of exogenous protein versus the endogenous (Figure 4H, lower panel).

The phosphorylation of eIF4GII maps to a novel N-terminal site

Previous work has established the presence of three serum sensitive serine phosphorylation sites on eIF4GI (Figure 5A) at 1148, 1188 and 1232 (using numbering for the longest eIF4GI isoform,[20, 21] with PKCα responsible for a further phosphorylation at Ser 1186[28]). In addition, CAMK1 has been described as phosphorylating eIF4GII (Figure 5D) in a similar C-terminal region of the molecule (Ser 1308[22]), using the numbering from our work which extended the N-terminus from a CUG initiation codon.[8]

To delineate the sites of phosphorylation observed in nocodazole treatment, we created cDNAs corresponding to regions of both proteins. Firstly, eIF4GI was separated into fragments corresponding to those that arise from caspase-directed cleavage of the protein during apoptosis. This separates the molecule into three "FAGs",[29-31] with each corresponding cDNA inserted into the same N-myc, C-3xFLAG vector as before. Each vector was then transfected into HeLa cells and 48 hours after transfection, the cells were incubated with or without nocodazole. Figure 5B shows that, there was a small, reproducible shift in only the N-terminal fragment (N-FAGf, lanes 1 and 2) and also more of the upper band in the doublet from C-FAG expressing cells. As two of the three known phosphoserines on eIF4GI are in this latter fragment, we concentrated our efforts on the N-FAGf, splitting it into further fragments, and carrying out experiments in a similar manner (Figure 5C). There was a slight shift in the f-QIAP and e-QIAP fragments, suggesting there may be a novel phosphorylation site between amino acids 41 and 147 (compare lane 1 with 2, and 3 with 4). However, this phosphorylation does not appear to be as robust as that observed in the full length protein and implies either that the protein must be intact or, more likely, that there are multiple sites present on eIF4GI and only when phosphorylated together is migration sufficiently retarded.

Our focus then turned to eIF4GII, with the N-terminus of this protein studied by again making cDNAs for insertion in the epitope-tagged vector (Figure 5D). In this case, there was a much clearer response to nocodazole treatment (Figure 5E), with a clear shift in migration of the MSGG-EELS (311-688) fragment (compare lanes 7 and 8). To map the site of modification, further fragments were constructed and examined in Figure 5F. While there was a perceptible shift in STVP-EELS, there was a much more obvious retardation of MSGG-AAPT (311-435) in nocodazole-treated cells (compare lanes 4 and 5). This subfragment was then subjected to immunoprecipitation by virtue of the C-terminal 3xFLAG tag, allowing us to examine the uppermost migrating species by mass spectroscopy and identify the site of modification.

Phosphorylation of eIF4GII occurs at two sites, with Cdk1 likely to be the kinase responsible for their modification

Mass spectrometric analysis of peptides generated from the MSGG-AAPT fragment identified two novel phosphorylation sites at Ser 384 and Ser 392 (Figure S2). These sites were aligned to the eIF4GI sequence (Figure 6A), which shows that they lie in a region of poor conservation and are hence unique to this paralogue. However, it is interesting to note that Ser 384 is a glutamic acid in eIF4GI

which suggests that the phosphorylation of this residue shifts the charge in this region of eIF4GII closer to that of eIF4GI. Our first task after making this identification was investigating whether alanine mutants of either of these sites would abrogate the nocodazole-dependent shift. Therefore site-directed mutagenesis was carried on one, the other, or both sites and the migration of these mutants and the wild type MSGG-APPT fragment were assayed as before (Figure 6B). The shift is no longer observed, but only in the double mutant (S384/392A), implying that both sites need to be phosphorylated to cause the shift, but there is no preference as to the order of modification.

Bioinformatic analysis using GPS 2.1.2[32] of the novel eIF4GII phosphorylation sites indicated that the most likely kinases responsible were Cdk1 and p38 MAPK. An experiment was therefore set up to investigate whether inhibitors of either kinase would abolish the nocodazole-dependent shift (Figure 6C). The modification was still evident in cells treated with the p38 MAPK inhibitor SB202190, but was lost in those treated with nocodazole and RO3306, the inhibitor of Cdk1. As the latter compound causes a synchronisation of the cells prior to the arrest induced by nocodazole treatment this result is perhaps not surprising. It therefore indicates that Cdk1 may be influencing the phosphorylation of eIF4GII either directly or indirectly, however this experiment does not offer definitive proof.

In vitro kinase assays were therefore undertaken to allow the direct phosphorylation of the MSGG-APPT fragment, which had been immunoprecipitated from asynchronous cells. In a “cold” kinase assay (Figure 6D), there is a slight mass increase in the upper band of the MSGG-AAPT fragment (compare lanes 1 and 2), giving direct evidence that Cdk1 is indeed the kinase responsible for phosphorylation of eIF4GII. However, in the context of this experiment the phosphorylation is nowhere near as robust as that observed with the same fragment expressed in HeLa cells exposed to nocodazole (lane 4).

Having confirmed the presence of novel phosphorylation sites in the N-terminus of eIF4GII, we finally wished to determine how they influenced the binding capacity of this scaffold protein in the context of the full length protein. The double S384/392A mutation was introduced into a vector which contained the full eIF4GII open reading frame arising from our recently identified CUG initiation codon, fused with a myc-tag at the N-terminus. This tag was then used to co-immunoprecipitate wild type or mutant eIF4GII from extracts from cells treated with or without nocodazole (Figure 6E). Extract from untransfected cells was also subjected to immunoprecipitation to ensure that any eluted proteins were present due to interaction with eIF4GII, not the agarose resin (lane 8). Due to the conditions of the assay, it was not possible to identify any eIF4A in the immunoprecipitation eluate, but PABP and eIF4E both co-eluted. Quantification of the ratios of eIF4GII or myc to either protein shows that there is a reduction in PABP binding on nocodazole treatment, which is much more severe in the S384/392A mutant. Given the proximity of the PABP binding site to the phosphorylated region, it is perhaps unsurprising that there is some influence on the interaction.

Subjecting the eluates to low percentage SDS-PAGE indicates that there is still some possible residual modification of the eIF4GII protein which contains the S384/392A mutant, indicating that there are other nocodazole-dependent phosphorylations elsewhere in the protein, as discussed below.

Discussion

Our work addresses some of the discrepancies that have been reported when observing cycling cells versus those that are arrested at various points in the cell cycle using pharmacological, nutritional or environmental treatments. The general consensus that there is a lack of protein synthesis during mitosis has come from the observation that treatment with colcemid, nocodazole or other microtubule disrupters (always for an extended period of time) results in a reduction in the incorporation of radiolabelled amino acids into precipitable proteins.[10, 16]

However, our work following cycling cells after release from a double thymidine block shows that there are no substantial changes in overall protein synthesis rates as measured by incorporation of radiolabelled amino acids (Figure 1). This is coupled with our observations that initiation factors and ribosomal proteins co-localise with tubulin at various points during mitosis (Figure 2) suggesting that ongoing translation is indeed important for the process. Previous work examining the protein content of isolated CHO cell midbodies also revealed the presence of other ribosomal proteins and translation elongation factors,[33] which supports our hypothesis that new proteins must be synthesised in order for proper abscission to proceed. Others have observed ribosomal protein S3 at the mitotic spindle[34] and suggested that this is due to the protein having a function in a process other than translation. However, given our observation of other ribosomal proteins and initiation factors at this location, we suggest that involvement in protein synthesis is more likely. The observation that rpS3 knockdown causes arrest in metaphase,[34] could also be interpreted as there being a key requirement for translation of mRNA during mitosis. Furthermore, our previous work examining the effects on cell morphology following knockdown of eIF4GI by shRNA[19] showed an uncoupling of karyokinesis from cytokinesis, resulting in production of large cells with multiple nuclei, with similar results observed when eIF3e/Int-6 was depleted from cells.[35] This phenotype is typically observed when similar experiments knock out or overexpress dominant negative forms of chromosomal passenger proteins (e.g. Aurora B, survivin[36]) suggesting these may be at least some of the particular components whose translation must be maintained during mitosis.

As there are well characterised interactions between cytoskeletal components and ribosomal proteins, translation initiation factors and various mRNPs,[37] it is therefore not surprising that using an agent such as nocodazole, which stops assembly of microtubules and also disassembles those previously made, should have such a drastic effect on protein synthesis. The link between cellular stress, the phosphorylation of eIF2 on Ser 51 of the α-subunit by one of four kinases and the consequential downregulation of translation rates has been comprehensively studied.[38] As others have previously observed, there is robust phosphorylation of eIF2α following incubation with nocodazole, and we also show that other components of the translation initiation machinery are phosphorylated. As phosphorylation of eIF2α still occurs in PKR-/- MEFs (Figure S1), these data indicate a role for PERK in modification of eIF2. Unfortunately, PERK -/- MEFs did not arrest with nocodazole and consequently showed no change in eIF2α phosphorylation.

The eIF4E-binding protein 4E-BP1 was observed to migrate as two forms, one corresponding to a completely unphosphorylated form (commonly referred to as the α form), whilst the other was retarded further in its migration compared to the gamma form which is phosphorylated at four sites (Thr 37, Thr 46, Ser 65 and Thr 70.[24] This led us to attempt to pinpoint the further sites of modification but our results mutating Thr 82, Ser 83 and Ser 112 proved inconclusive. Advances in

the sensitivity of proteomic instrumentation has led several groups to undertake large-scale phosphoproteomic analysis of cells (including HeLa cells) treated with nocodazole. For example, a recent publication involving HEK293 cells found a further 11 sites of phosphorylation over the standard four, which included Ser 83 and Ser 112.[39] Given that the shift in migration we observe does not correspond to such a drastic change in phosphorylation, which would result in multiple species on an immunoblot, it is possible that a single 4E-BP1 protein only undergoes some but not all possible modifications, in a particularly disorganised manner. In addition, how some 4E-BP1 protein remains in a completely unphosphorylated state is an as yet unanswered question. This could reflect some sort of protection in a compartment or complex which is inaccessible to the kinase(s) activated upon sustained incubation with nocodazole. It is also feasible that only pre-phosphorylated forms of 4E-BP1 can then undergo further modifications, analogous to the observation that only phosphorylated 4E-BP1 is subjected to ubiquitination.[40, 41]

Our investigations of the eIF4G paralogues were successful in identifying two sites of phosphorylation on eIF4GII at Ser 384 and Ser 392, through a combination of deletion analysis and unphosphorylatable serine-alanine mutations. While we have not conclusively identified the kinase responsible for this modification, it does appear likely to be Cdk1. The larger scale study of HEK293 cells treated with nocodazole independently confirmed these modifications and also indicates several others, including one at Ser 382, one at Ser 644 (so may be evident when comparing Figure 5E, lanes 8 and 9) and another at Ser 1560. A caveat of this previously published work is that, due to the experimental design, no distinction can be made between those residues which were phosphorylated in response to nocodazole or already modified. However, of particular interest was a phosphothreonine residue identified in the extended N-terminus, initiated from a CUG which is completely absent in eIF4GI proteins; the analysis could not determine whether Thr 64 or Thr 66 was the amino acid in question. This particular modification could account for the altered banding pattern observed above the main band in Figure 5E, lane 4.

This comprehensive study did not identify any phosphopeptides in eIF4GI although an earlier independent study[42] did find phosphorylation of this paralogue at both known sites (Ser 1186 and Ser 1188), together with another at Ser 1232. All these sites reside in the C-FAG fragment of eIF4GI and again could reflect the alteration in intensity of the two bands observed in Figure 5B, comparing lanes 5 and 6.

The sites that we and others have identified in eIF4GII are between the regions known to bind PABP and eIF4E, which is notable as being the most poorly conserved region and lacks any currently unassigned binding partners in either paralogue (Figures 5A and 5D). Our previous work identified a nuclear localisation signal in eIF4GI further downstream of this region, which is not present in eIF4GII.[17] Taken together these findings confirm that, despite initial experiments showing that the paralogues were functionally interchangeable, they are subject to several alternative regulatory controls. We have not been able to identify any clear changes in the composition of the eIF4F complex in response to these modifications, but they may be acting functionally somewhere else in the initiation pathway other than during the assembly of the mRNA-binding complex of eIF4E:eIF4G:PABP.

It is clear from our work and the larger scale phosphoproteomic surveys that a number of initiation factors are modified by kinases following sustained nocodazole treatment, with the general

consequence that translation rates are significantly reduced. However, as others have previously shown,[16] a subset of messages is maintained in actively translating pools, with IRES-dependent translation postulated to be responsible for maintaining their translation while general cellular messages are inhibited. Different IRESs have alternative requirements for the canonical initiation factor machinery and it would be interesting to determine the eIF4G requirement and which particular modifications exert effects on IRES-driven translation.

For a cell to progress through mitotis, a plethora of regulated phosphorylation and dephosphorylation events must occur.[43] Our work has demonstrated increases in phosphorylation of key translation initiation factors following nocodazole treatment, which arrests cells at the G_2/M boundary. However, when adding nocodazole for shorter times, these modifications were not observed. This suggests either that phosphorylation is a consequence of prolonged incubation which may activate further stress pathways, or that phosphorylation is extremely transient and only perceivable when given the opportunity to accumulate in stalled cells. While it is still not clear why these modifications are specifically required for mitotic progression, they do show that there is still much to learn about phosphorylation of initiation factors in different cellular conditions. Given that there is a considerable amount of research into using microtubule and other cytoskeletal disruptors as chemotherapeutic agents,[44-47] it is important to consider how these treatments may also be impinging upon gene expression at the level of translation initiation.

Materials and Methods:

Cell Culture and transient transfection Materials for tissue culture were from Invitrogen (UK) and foetal bovine serum (FBS) was from Labtech International (UK) or Invitrogen. HeLa (cervical cancer) cells were obtained from the ECACC (Salisbury, UK) and maintained in DMEM supplemented with 10% FBS at 37°C in a humidified atmosphere containing 5% CO_2.

Cell cycle synchronisation of HeLa cells was carried out following conditions as described by others.[15] Briefly, for the double thymidine block, cells were incubated for 16 hours with 2 mM thymidine, released for 8 hours, then synchronised for a further 16 hours with 2mM thymidine. For the thymidine/nocodazole treatments, the cells were incubated for 16 hours with 2mM thymidine, released for 6 hours, then incubated in 0.6µg/ml nocodazole for 20 hours.

For transient transfection cells were seeded on 6 cm plates at a density of $1x10^5$ cells per plate and 24h later cells were transfected with 1 µg of pcDNA plasmid using GeneJuice (Merck, UK http://www.merckmillipore.com/united-kingdom/chemicals/genejuice-transfection-reagent/EMD_BIO-70967/p_qI6b.s1OxjIAAAEjOhx9.zLX?PortalCatalogID=merck4biosciences), according to the manufacturer's protocol. The transfection mixture was removed 24h later, and the cells were washed twice with PBS and further incubated in fresh media for 24h, until the addition of nocodazole . Preparation of cell lysates, and measurement of protein synthesis rates by incorporation of [^{35}S] methionine into protein were carried out as previously described.[19] Cell extracts were also prepared using M-PER reagent (Pierce http://www.piercenet.com/browse.cfm?fldID=06010420), supplemented with Halt phosphatase and protease inhibitor cocktail (Pierce http://www.piercenet.com/browse.cfm?fldID=E780097B-5056-8A76-4EFC-572566DA6E04), as per the manufacturer's instructions.

Plasmids pcDNA plasmids containing N-terminal myc tags and C-terminal 3xFLAG tags have been described previously.[8, 17, 19] For this study, cDNAs corresponding to portions of eIF4GI/II or 4E-BP1 were subcloned from existing plasmids or HeLa cell cDNA using appropriate primers to maintain the open reading frame with the epitope tags, removing any endogenous stop codons where necessary. Site directed mutagenesis to generate alanine mutations of phosphorylation sites was performed using the Agilent Quikchange Lightning kit (http://www.genomics.agilent.com/en/product.jsp?cid=AG-PT-175&tabId=AG-PR-1162&_requestid=640783) in accordance with the manufacturer's instructions, using primers synthesised as directed by the Agilent Quikchange Primer design program. All sequences were confirmed by automated sequencing (Eurofins MWG or Beckman Coulter Genomics).

FACS analysis At each time point, to ensure all cells both adherent and in suspension were harvested, all growth medium was removed and combined with a single PBS wash and the remaining cells which were subsequently harvested from the plate by dissociation with trypsin. Following centrifugation (1000xg for 5 min) and a single wash with ice-cold PBS, cells were fixed in 3ml of freshly made ice-cold 70% EtOH, 30% PBS and left at 4°C overnight. Each sample was washed twice in PBS before being resuspended in 500 µl PBS, containing 0.1 mg/ml RNase A to digest RNA and 0.03 mg/ml Propidium Iodide solution to stain DNA, prior to incubation at RT for 30 min. Samples were analysed with a BD FACScan™ using appropriate filter sets.

Immunoblotting Antibodies to eIF4GI, eIF4GII, eIF4A, eIF4E and PABP were prepared in house and have been previously described.[17, 19] Antibodies to total 4E-BP1 http://www.cellsignal.com/products/9452.html, phospho-4E-BP1 (Ser65) http://www.cellsignal.com/products/9451.html, phosphor-4E-BP1 (Thr70) http://www.cellsignal.com/products/9455.html, total eIF2α http://www.cellsignal.com/products/9722.html and phospho-eIF2α http://www.cellsignal.com/products/9721.html were from Cell Signaling Technology. Antibodies to myc (9E10) http://www.sigmaaldrich.com/catalog/product/sigma/m4439?lang=en&region=GB FLAG (M2) http://www.sigmaaldrich.com/catalog/product/sigma/f1804?lang=en&region=GB and actin http://www.sigmaaldrich.com/catalog/product/sigma/a2668?lang=en&region=GB were from Sigma-Aldrich.

Polysome gradients Sucrose density gradients to separate ribosomal subunits and those ribosomes associated with mRNAs were carried out as previously described.[48]

Isolation of protein complexes from cell extracts m^7GTP-Sepharose affinity isolation of eIF4E and associated factors, were carried out as previously described.[19] Immunoprecipitation and Co-immunoprecipitation experiments were carried out using the Pierce Co-Immunoprecipitation kit http://www.piercenet.com/browse.cfm?fldID=AB59D109-9690-4EAA-8521-E6C407156407, as per the manufacturer's instructions, with anti-myc 9E10 or anti-FLAG M2 immobilised to the resin, depending on the experiment.

Mass spec analysis FLAG-tagged immunoprecipitated protein was firstly separated by 1D-SDS-PAGE using a precast Novex Bis-Tris 4-12% gel http://www.invitrogen.com/site/us/en/home/Products-and-Services/Applications/Protein-Expression-and-Analysis/Protein-Gel-Electrophoresis/Protein-Gels/Novex-NuPAGE-SDS-PAGE-Gels/NuPAGE-SDS-PAGE-Bis-Tris-Gel.html. Following staining with Colloidal Coomassie blue, the gel band of interest was subjected to in-situ trypsin digestion using the

method of Schevchenko et al.[49] Peptide extracts were enriched for phosphopeptides using TiO_2 ProteaTips (Protea Biosciences, WV USA https://proteabio.com/products/SP-125) and used in accordance with the manufacturer's instructions. Lyophilised peptide samples were re-suspended in 50 mM sodium citrate pH 6.0 and loaded onto a reverse phase trap column (Symmetry C18, 5 µm, 180 µm x 20mm, Waters Corporation http://www.waters.com/waters/en_GB/Symmetry-Columns/nav.htm?cid=513219&locale=en_GB), at a flow rate of 5 µl/min and washed for 10 minutes with 3% acetonitrile containing 0.1% formic acid (buffer A) prior to the analytical nano-LC separation using a C18 Reverse phase column (HSS T3, 1.8 µm, 200mm x 75µm, Waters http://www.waters.com/waters/en_GB/HSS-%28High-Strength-Silica%29Technology/nav.htm?cid=134618105). Separation of peptides was achieved using a gradient of 0-50% buffer B (95% acetonitrile containing 0.1% formic acid (v/v)) at a flow rate of 300 nl/min. Eluted samples were sprayed directly into a Synapt G2-S mass spectrometer (Waters, Manchester, UK) operating in MSe mode. Data was acquired from 50 to 2000 m/z using alternate low and high collision energy (CE) scans. Low CE was 5V and elevated collision energy ramp from 15 to 40V. Ion mobility was implemented prior to fragmentation using a wave velocity of 650 m/s and wave height of 40V. The lock mass Glu-fibrinopeptide, ((M+2H)+2, m/z = 785.8426) was infused at a concentration of 100 fmol/µl with a flow rate of 250 nl/min and acquired every 60 seconds.

The raw mass spectra were submitted to ProteinLynx Global Server version 2.5.2 (Waters, Manchester, UK), and the data processed to generate reduced charge state and deisotoped precursor and associated product ion mass lists. These mass lists were searched against the human UniProt protein sequence database (August, 2012) using the MASCOT search algorithm. A maximum of one missed cleavage was allowed for tryptic digestion with a fixed modification of carboxyamidomethylation of cysteines and variable modifications set to allow for oxidation of methionine and the phosphorylation of serine, threonine and tyrosine.

Precursor ion and sequence ion mass tolerances were set at 20 ppm and 0.25 Da, respectively. The significance threshold for search results was set at $p<0.05$.

Kinase assays Recombinant Cdk1/cyclinB1 was purchased from New England Biolabs https://www.neb.com/products/p6020-cdk1-cyclin-b, and the fragment of eIF4GII was obtained from an IP eluate and phosphorylated with 10 units of kinase for 30 minutes at 30°C in the presence of 200 µM ATP, in accordance with the manufacturer's instructions. Enzyme activity was confirmed in parallel experiments by phosphorylation of eEF2K[50] in the presence of 200 µM unlabelled ATP and 1 µCi of [γ-32P] ATP.

Acknowledgments

We would like to thank the Biotechnology and Biological Sciences Research Council (grant numbers BB/D007593/1 and BB/H006834/1) for funding this work. LSP is funded by a BBSRC doctoral training studentship. Thanks to Paul Skipp and Erika Parkinson from the Centre for Proteomics Research, University of Southampton for their help with the mass spectroscopy, to Claire Moore for assistance with kinase assays and to Natalie Hudson and Zoe Davies for initial work on constructing deletion fragments of eIF4GI and II.

References

1. Jackson RJ, Hellen CU, Pestova TV. The mechanism of eukaryotic translation initiation and principles of its regulation. Nat Rev Mol Cell Biol 2010; 11:113-27.
2. Laplante M, Sabatini DM. mTOR signaling in growth control and disease. Cell 2012; 149:274-93.
3. Ma XM, Blenis J. Molecular mechanisms of mTOR-mediated translational control. Nat Rev Mol Cell Biol 2009; 10:307-18.
4. Morley SJ, Coldwell MJ, Clemens MJ. Initiation factor modifications in the preapoptotic phase. Cell Death Differ 2005; 12:571-84.
5. Proud CG. mTOR Signalling in Health and Disease. Biochem Soc Trans 2011; 39:431-6.
6. Sonenberg N, Hinnebusch AG. Regulation of translation initiation in eukaryotes: mechanisms and biological targets. Cell 2009; 136:731-45.
7. Gradi A, Imataka H, Svitkin YV, Rom E, Raught B, Morino S, et al. A novel functional human eukaryotic translation initiation factor 4G. Mol Cell Biol 1998; 18:334-42.
8. Coldwell MJ, Sack U, Cowan JL, Barrett RM, Vlasak M, Sivakumaran K, et al. Multiple isoforms of the translation initiation factor eIF4GII are generated via use of alternative promoters, splice sites and a non-canonical initiation codon. Biochem J 2012; 448:1-11.
9. Tinton SA, Schepens B, Bruynooghe Y, Beyaert R, Cornelis S. Regulation of the cell-cycle-dependent internal ribosome entry site of the PITSLRE protein kinase: roles of Unr (upstream of N-ras) protein and phosphorylated translation initiation factor eIF-2alpha. Biochem J 2005; 385:155-63.
10. Fan H, Penman S. Regulation of protein synthesis in mammalian cells. J Mol Biol 1970; 50:655-70.
11. Pyronnet S, Dostie J, Sonenberg N. Suppression of cap-dependent translation in mitosis. Genes Dev 2001; 15:2083-93.
12. Pyronnet S, Sonenberg N. Cell cycle-dependent translational control. Curr Opin Genet Dev 2001; 11:13-8.
13. Bonneau AM, Sonenberg N. Involvement of the 24-kDa cap-binding protein in regulation of protein synthesis in mitosis. J Biol Chem 1987; 262:11134-9.
14. Heesom KJ, Gampel A, Mellor H, Denton RM. Cell cycle-dependent phosphorylation of the translational repressor eIF-4E binding protein-1 (4E-BP1). Curr Biol 2001; 11:1374-9.
15. Whitfield ML, Sherlock G, Saldanha AJ, Murray JI, Ball CA, Alexander KE, et al. Identification of genes periodically expressed in the human cell cycle and their expression in tumors. Mol Cell Biol 2002; 13:1977-2000.
16. Qin X, Sarnow P. Preferential translation of internal ribosome entry site containing mRNAs during the mitotic cell cycle in mammalian cells. J Biol Chem 2004; 279:13721-8.
17. Coldwell MJ, Hashemzadeh-Bonehi L, Hinton TM, Morley SJ, Pain VM. Expression of fragments of translation initiation factor eIF4GI reveals a nuclear localisation signal within the N-terminal apoptotic cleavage fragment N-FAG. J Cell Sci 2004; 117:2545-55.
18. Margalit A, Vlcek S, Gruenbaum Y, Foisner R. Breaking and making of the nuclear envelope. J Cell Biochem 2005; 95:454-65.
19. Coldwell MJ, Morley SJ. Specific isoforms of translation initiation factor 4GI show differences in translational activity. Mol Cell Biol 2006; 26:8448-60.
20. Bradley CA, Padovan JC, Thompson TC, Benoit CA, Chait BT, Rhoads RE. Mass spectrometric analysis of the N-terminus of translation initiation factor eIF4G-1 reveals novel isoforms. J Biol Chem 2002; 277:12559-71.
21. Byrd MP, Zamora M, Lloyd RE. Generation of multiple isoforms of eukaryotic translation initiation factor 4GI by use of alternate translation initiation codons. Mol Cell Biol 2002; 22:4499-511.

22. Qin H, Raught B, Sonenberg N, Goldstein EG, Edelman AM. Phosphorylation screening identifies translational initiation factor 4GII as an intracellular target of Ca(2+)/calmodulin-dependent protein kinase I. J Biol Chem 2003; 278:48570-9.
23. Vassilev LT, Tovar C, Chen S, Knezevic D, Zhao X, Sun H, et al. Selective small-molecule inhibitor reveals critical mitotic functions of human CDK1. Proc Natl Acad Sci U S A 2006; 103:10660-5.
24. Gingras AC, Gygi SP, Raught B, Polakiewicz RD, Abraham RT, Hoekstra MF, et al. Regulation of 4E-BP1 phosphorylation: a novel two-step mechanism. Genes Dev 1999; 13:1422-37.
25. Gingras AC, Raught B, Gygi SP, Niedzwiecka A, Miron M, Burley SK, et al. Hierarchical phosphorylation of the translation inhibitor 4E-BP1. Genes Dev 2001; 15:2852-64.
26. Fadden P, Haystead TA, Lawrence JC, Jr. Identification of phosphorylation sites in the translational regulator, PHAS-I, that are controlled by insulin and rapamycin in rat adipocytes. J Biol Chem 1997; 272:10240-7.
27. Heesom KJ, Avison MB, Diggle TA, Denton RM. Insulin-stimulated kinase from rat fat cells that phosphorylates initiation factor 4E-binding protein 1 on the rapamycin-insensitive site (serine-111). Biochem J 1998; 336 (Pt 1):39-48.
28. Dobrikov M, Dobrikova E, Shveygert M, Gromeier M. Phosphorylation of eukaryotic translation initiation factor 4G1 (eIF4G1) by protein kinase C{alpha} regulates eIF4G1 binding to Mnk1. Mol Cell Biol 2011; 31:2947-59.
29. Bushell M, Poncet D, Marissen WE, Flotow H, Lloyd RE, Clemens MJ, et al. Cleavage of polypeptide chain initiation factor eIF4GI during apoptosis in lymphoma cells: characterisation of an internal fragment generated by caspase-3-mediated cleavage. Cell Death Differ 2000; 7:628-36.
30. Clemens MJ, Bushell M, Morley SJ. Degradation of eukaryotic polypeptide chain initiation factor (eIF) 4G in response to induction of apoptosis in human lymphoma cell lines. Oncogene 1998; 17:2921-31.
31. Marissen WE, Lloyd RE. Eukaryotic translation initiation factor 4G is targeted for proteolytic cleavage by caspase 3 during inhibition of translation in apoptotic cells. Mol Cell Biol 1998; 18:7565-74.
32. Xue Y, Ren J, Gao X, Jin C, Wen L, Yao X. GPS 2.0, a tool to predict kinase-specific phosphorylation sites in hierarchy. Molecular & cellular proteomics : MCP 2008; 7:1598-608.
33. Skop AR, Liu HB, Yates J, Meyer BJ, Heald R. Dissection of the mammalian midbody proteome reveals conserved cytokinesis mechanisms. Science 2004; 305:61-6.
34. Jang CY, Kim HD, Zhang X, Chang JS, Kim J. Ribosomal protein S3 localizes on the mitotic spindle and functions as a microtubule associated protein in mitosis. Biochem Biophys Res Commun 2012; 429:57-62.
35. Morris C, Jalinot P. Silencing of human Int-6 impairs mitosis progression and inhibits cyclin B-Cdk1 activation. Oncogene 2005; 24:1203-11.
36. Carmena M, Wheelock M, Funabiki H, Earnshaw WC. The chromosomal passenger complex (CPC): from easy rider to the godfather of mitosis. Nat Rev Mol Cell Biol 2012; 13:789-803.
37. Kim S, Coulombe PA. Emerging role for the cytoskeleton as an organizer and regulator of translation. Nat Rev Mol Cell Biol 2010; 11:75-81.
38. Wek RC, Jiang HY, Anthony TG. Coping with stress: eIF2 kinases and translational control. Biochem Soc Trans 2006; 34:7-11.
39. Franz-Wachtel M, Eisler SA, Krug K, Wahl S, Carpy A, Nordheim A, et al. Global detection of protein kinase D-dependent phosphorylation events in nocodazole-treated human cells. Molecular & cellular proteomics : MCP 2012; 11:160-70.
40. Elia A, Constantinou C, Clemens MJ. Effects of protein phosphorylation on ubiquitination and stability of the translational inhibitor protein 4E-BP1. Oncogene 2008; 27:811-22.
41. Clemens MJ, Coldwell M, Elia A. EIF4EBP1 (Eukaryotic translation initiation factor 4E binding protein 1). Atlas Genet Cytogenet Oncol Haematol 2012.

42. Nagano K, Shinkawa T, Mutoh H, Kondoh O, Morimoto S, Inomata N, et al. Phosphoproteomic analysis of distinct tumor cell lines in response to nocodazole treatment. Proteomics 2009; 9:2861-74.
43. Wurzenberger C, Gerlich DW. Phosphatases: providing safe passage through mitotic exit. Nat Rev Mol Cell Biol 2011; 12:469-82.
44. Perez EA. Microtubule inhibitors: Differentiating tubulin-inhibiting agents based on mechanisms of action, clinical activity, and resistance. Molecular cancer therapeutics 2009; 8:2086-95.
45. Harrison MR, Holen KD, Liu G. Beyond taxanes: a review of novel agents that target mitotic tubulin and microtubules, kinases, and kinesins. Clinical advances in hematology & oncology : H&O 2009; 7:54-64.
46. Pasquier E, Kavallaris M. Microtubules: a dynamic target in cancer therapy. IUBMB life 2008; 60:165-70.
47. Singh P, Rathinasamy K, Mohan R, Panda D. Microtubule assembly dynamics: an attractive target for anticancer drugs. IUBMB life 2008; 60:368-75.
48. Hinton TM, Coldwell MJ, Carpenter GA, Morley SJ, Pain VM. Functional analysis of individual binding activities of the scaffold protein eIF4G. J Biol Chem 2007; 282:1695-708.
49. Shevchenko A, Jensen ON, Podtelejnikov AV, Sagliocco F, Wilm M, Vorm O, et al. Linking genome and proteome by mass spectrometry: large-scale identification of yeast proteins from two dimensional gels. Proc Natl Acad Sci U S A 1996; 93:14440-5.
50. Smith EM, Proud CG. cdc2-cyclin B regulates eEF2 kinase activity in a cell cycle- and amino acid-dependent manner. EMBO J 2008; 27:1005-16.

Figure legends:

Figure 1. Protein synthesis rates are *not d*ecreased during M phase when observing cycling synchronised cells.

(A) Exponentially growing HeLa cells were maintained as an asynchronous population or synchronised at the G_1/S boundary by double thymidine block and released for the number of hours indicated. Nuclei content of cells at each time point was determined by staining with propidium iodide and FACS analysis.

(B) In parallel experiments translation rates were examined by pulsing cells with ^{35}S Methionine for 30 minutes prior to harvest. Extracts were prepared, and the incorporation of radioactive methionine into protein (cpm/μg total protein) determined as described in the text. For the T/N sample, HeLa cells were blocked once in thymidine before being released then synchronised in M phase by incubation with the microtubule depolymerizing agent nocodazole for 19 hours.

(C) Equal amounts of extract from (B) were subjected to SDS-PAGE and proteins transferred to PVDF. The membrane was then probed with the antibodies shown and visualized with secondary antibodies conjugated to HRP.

Figure 2. The translation machinery costains with the microtubule network during different stages of mitosis and cytokinesis

Cells released from a double thymidine block for 9 hours were fixed with 4% (w/v) paraformaldehyde and permeabilised with 0.1% (v/v) Triton X-100. Cells in different stages of mitosis and cytokinesis were examined by confocal microscopy, as determined by the positioning of microtubules or DNA (A-E). Upper panels show components of the translation machinery which were detected with rabbit polyclonal antibodies, as indicated, followed by an anti-rabbit secondary antibody conjugated to Alexa Fluor 555 (red). Lower panels show this signal merged with α-tubulin detected with a mouse monoclonal antibody conjugated to FITC (green) and DNA detected with DAPI (blue).

Figure 3. Synchronisation with nocodazole inhibits translation and leads to substantial phosphorylation of components of the translation initiation machinery

(A) HeLa cells were either maintained asynchronously, or blocked once in thymidine before being released then synchronised in M phase by incubation with the microtubule depolymerizing agent nocodazole for 19 hours. As before, FACS analysis was used to determine nuclear DNA content.

(B) Samples were subjected to sucrose density gradient centrifugation to determine the effect of incubation with nocodazole on polysome formation. Translation rates from these cells are shown as part of Figure 1(B), which confirm the large inhibition of translation, as determined by the reduction in 35S methionine incorporation.

(C) Equal amounts of cell extracts from parallel samples were analysed by immunoblotting for the proteins indicated. To separate isoforms of eIF4G proteins that arise from alternative translation initiation, low percentage SDS-PAGE was used.

(D) To determine whether shifts in migration of eIF4GI/II and 4E-BP1 were due to phosphorylation, extracts from asynchronous cells or cells which had been incubated with nocodazole for 19 hours were prepared. These were then incubated in the presence or absence of lambda protein phosphatase for 30 minutes before the treated extracts were separated by SDS-PAGE and immunoblotted for the indicated proteins.

Figure 4. Robust phosphorylation of eIF2α does not occur following release from G_2/M block and arresting synchronous cells with nocodazole has negligible effects on translation rates

(A) HeLa cells were maintained asynchronously, subjected to a single thymidine nocodazole block, or incubated with the Cdk1 inhibitor RO3306 for 20 hours at a concentration of 9 μM to arrest cells at the end of G_2. As this latter inhibitor is reversible, the drug was washed off and the cells progressed through mitosis, as observed by FACS analysis every 30 min.

(B) Translation rates (obtained by pulsing for 15 min prior to harvest) were obtained from parallel experiments to (A)

(C) Mobility shifts of eIF4GI and 4E-BP1 and the phosphorylation status of eIF2α were determined from cell extracts prepared in (C) by SDS-PAGE and immunoblotting with antibodies raised against standard or phosphor-epitopes, as indicated.

(D) Cells were synchronised with a double thymidine block as before, then released into either medium which was either normal, supplemented with nocodazole at release, or supplemented with nocodazole 6 hours after release. FACS analysis of cells at the timepoints shown was used to show the arrest in G_2/M in the cells incubated with nocodazole.

(E) The amount of incorporation of [^{35}S] methionine into protein for the 15 minutes prior to harvest was determined from parallel experiments to (D) as previously described.

(F) As before, cell extracts from parallel experiments to (D) were made and subjected to SDS-PAGE and immunoblotting to show the phosphorylation status of eIF2α and 4E-BP1 in the three different treatments.

(G) In an attempt to determine the novel phosphorylation site of 4E-BP1 that is detected following nocodazole treatment, the open reading frame of human protein was inserted into a vector, in frame with an N-terminal myc-tag and C-terminal 3xFLAG tag. Further variants were constructed where putative phosphorylation sites (S83 and S112) were mutated to alanine either singly or in combination. The four variants were then transfected into HeLa cells and either maintained asynchronously or treated with nocodazole for 19h. Cell extracts were prepared and the migration of the exogenous proteins determined by SDS-PAGE, detected with anti-FLAG antibody.

(H) As for (G) mutants of 4E-BP1 were prepared where putative phosphorylation sites (T82 and S83) were mutated to alanine. After transfection into HeLa cells and nocodazole treatment as before, migration of FLAG-tagged proteins was examined by immunoblotting.

Figure 5. Deletion analysis of eIF4G proteins reveals two novel phosphoserine sites in eIF4GII

(A) A schematic representation of eIF4GI, showing the alternative AUG translation initiation sites (f through a) and the caspase-3 cleavage sites used to generate deletion fragments of this protein. Numbering conforms to the longest isoform as independently identified by others [20, 21]. Each cDNA was inserted into a vector containing an N-terminal myc-tag and C-terminal 3xFLAG tag to enable detection.

(B) Plasmids containing cDNAs representing the three fragments of apoptotic cleavage of eIF4GI (FAGs) were transfected into HeLa cells either untreated or incubated with nocodazole for 19h. Any changes in migration of the fragments due to the presence of nocodazole was determined by SDS-PAGE and immunoblotting using anti-FLAG antibody to detect fragment expression.

(C) Further deletion fragments of N-FAGf were constructed as before to delineate regions likely to be phosphorylated, these were transfected into HeLa cells and migration in the presence or absence of nocodazole was examined.

(D) Deletion fragments of the N-terminus of eIF4GII were constructed as before, in order to map the phosphorylation site(s) of this protein. The amino acid numbering conforms to the CUGb initiated isoform previously identified by our group [8], which extends the open reading frame N-terminally from the initially published AUG.

(E) Migration of the N-terminal fragments was examined following treatment with nocodazole for 19h, with proteins detected with anti-FLAG antibody.

(F) Further subfragments were made of the eIF4GII open reading frame, as indicated in (D), and their migration in cells treated with nocodazole determined as before.

Figure 6. Identification of phosphorylation of eIF4GII at S385 and S389 by Cdk1, and consequences for initiation factor complex formation

(A) Mass spectroscopy was used to identify phosphorylation of two serine residues (384 and 392) within the MSGG-APPT fragment of eIF4GII following immunoprecipitation of the fragment from cells treated with nocodazole. The sites are shown in bold and underlined, and the surrounding sequences were aligned with eIF4GI using CLUSTALW, showing the poor conservation of this particular region of the protein. The site of PABP binding is shown in grey, with a dashed underline. The symbols * : and . respectively denote identical residues, or conserved and semi-conserved substitutions in the alignment.

(B) Ser-Ala mutants, either single or in combination, of the MSGG-APPT fragment of eIF4GII were made and inserted into the myc-3xFLAG vector as before. Cells transfected with these vectors were incubated with or without nocodazole and migration of the proteins examined as before.

(C) Prediction software (GPS 2.1.2) indicated that likely kinases responsible for this phosphorylation were p38 MAPK or Cdk1. Therefore cell extracts were made from cells transfected with MSGG-APPT that had been incubated with or without nocodazole and cell permeable kinase inhibitors. These would either block p38 MAPK signalling (SB202190) or Cdk1 signalling (RO3306). Migration of the eIF4GII fragment was determined as previously described.

(D) To confirm the results from panel (C), immunoprecipitated MSGG-AAPT protein was incubated in the presence of recombinant Cdk1/cyclin B and ATP. This was run alongside a positive control of extract from cells treated with or without nocodazole.

(E) To determine whether the novel phosphorylation sites have any influence on the interactions of eIF4GII with other components of the translation initiation factor machinery, the S384/392A double mutant was introduced into the full length eIF4GII CUGb ORF. This vector contains an N-terminal myc tag, and therefore exogenous eIF4GII could be immunoprecipitated from transfected cells which had been incubated with nocodazole. The left hand panel shows the levels of endogenous proteins as determined by SDS-PAGE and immunoblotting, and the right hand panel shows the eluate from a co-immunoprecipitation where myc-9E10 antibody had been captured on agarose resin.

Figure S1. PKR is not responsible for phosphorylation of eIF2α and hyperphosphorylation of 4E-BP1 is mTORC1-independent.

Mouse embryonic fibroblasts from PKR–/– animals (a kind gift from Prof. C. Weissmann) were incubated with thymidine for 16 hours, released for 4 hours, preincubated with various kinase inhibitors for 1 hour, then incubated without (left panel) or with nocodazole (right panel) for 16 hours.

Phosphorylation of eIF2α and modification of 4E-BP1 still occurred in cells treated with nocodazole alone. These events are not observed in cells treated with U0126 or RO-3306, but these inhibitors are known to arrest cells in G_2, therefore the cells did not progress to M phase. The upwards shift of 4E-BP1 in the presence of nocodazole is still observed in cells treated with Rad001, suggesting mTORC1 signalling is not involved in this modification.

Figure S2. Raw mass spectra of eIF4GII phosphopeptides.

Cells were transfected with a pcDNA plasmid expressing the eIF4GII MSGG-AAPT fragment (Figure 5D), respectively tagged at the N- and C-termini with myc and 3XFLAG epitope tags. Cell extracts were prepared from control asynchronous cells and cells treated with nocodazole as before. The extracts were subjected to immunoprecipitation with an anti-FLAG M2 monoclonal antibody and the eluted proteins were separated by SDS-PAGE. Coomassie staining was used to visualise the eluted proteins and the bands that were present only in the nocodazole treated lane (as per Figure 5F) were excised, eluted and subjected to mass spectroscopy to identify phosphopeptides.

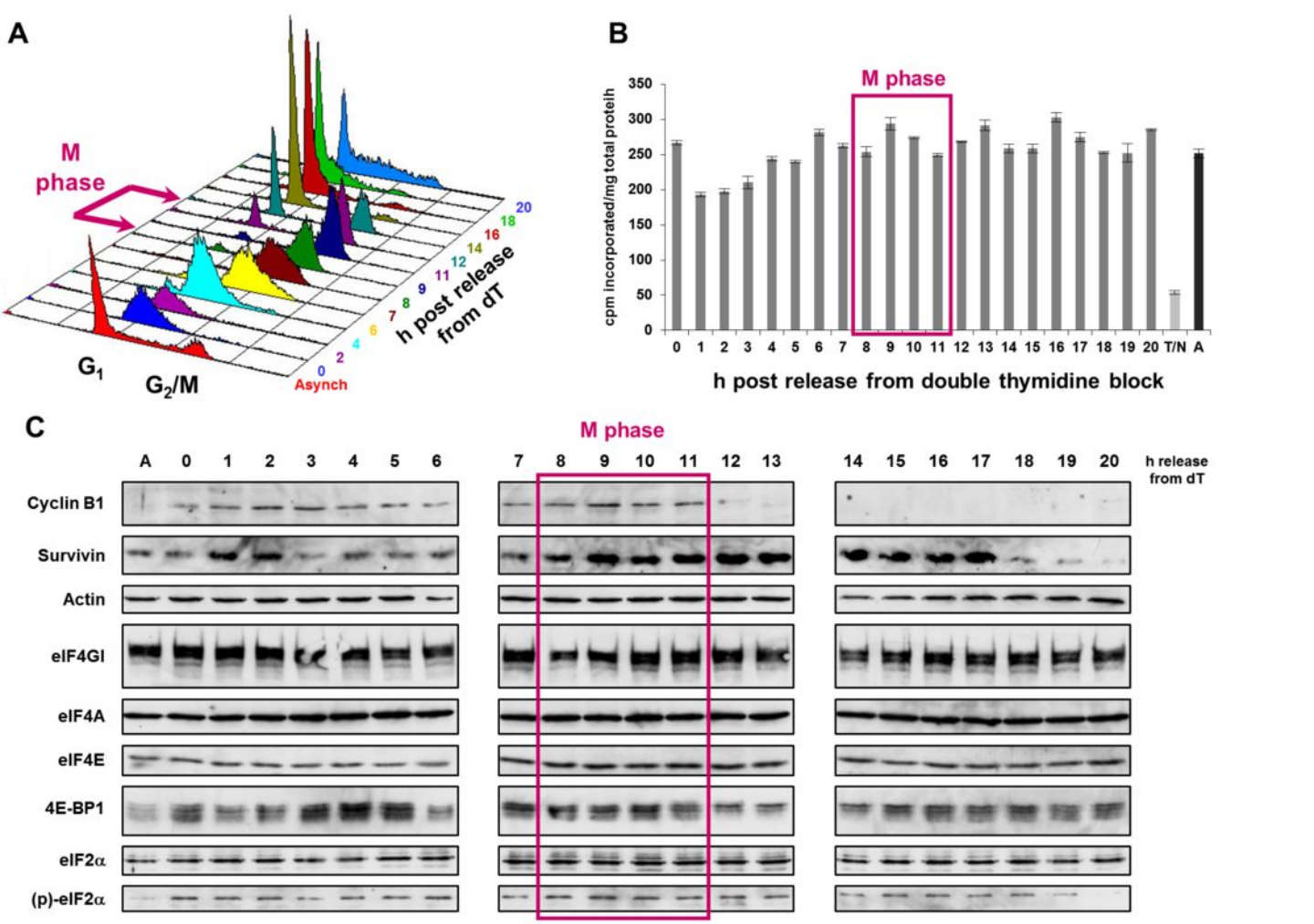
A
M phase
G1
G2/M
Asynch
h post release from dT
B
M phase
cpm incorporated/mg total proteih
h post release from double thymidine block
C
M phase
h release from dT
Cyclin B1
Survivin
Actin
eIF4GI
eIF4A
eIF4E
4E-BP1
eIF2α
(p)-eIF2α

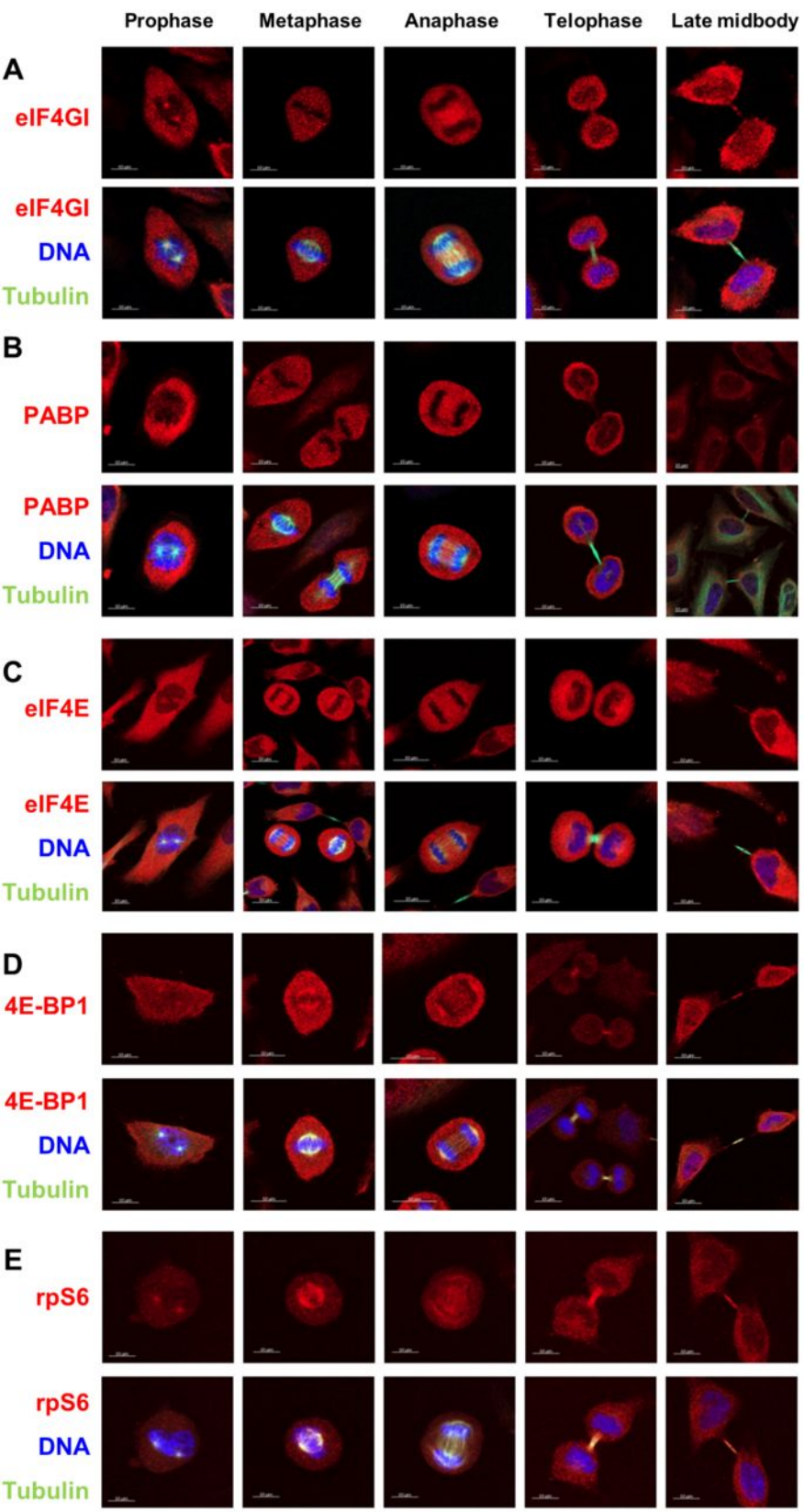
Prophase
Metaphase
Anaphase
Telophase
Late midbody
A
eIF4GI
eIF4GI
DNA
Tubulin
B
PABP
PABP
DNA
Tubulin
C
eIF4E
eIF4E
DNA
Tubulin
D
4E-BP1
4E-BP1
DNA
Tubulin
E
rpS6
rpS6
DNA
Tubulin

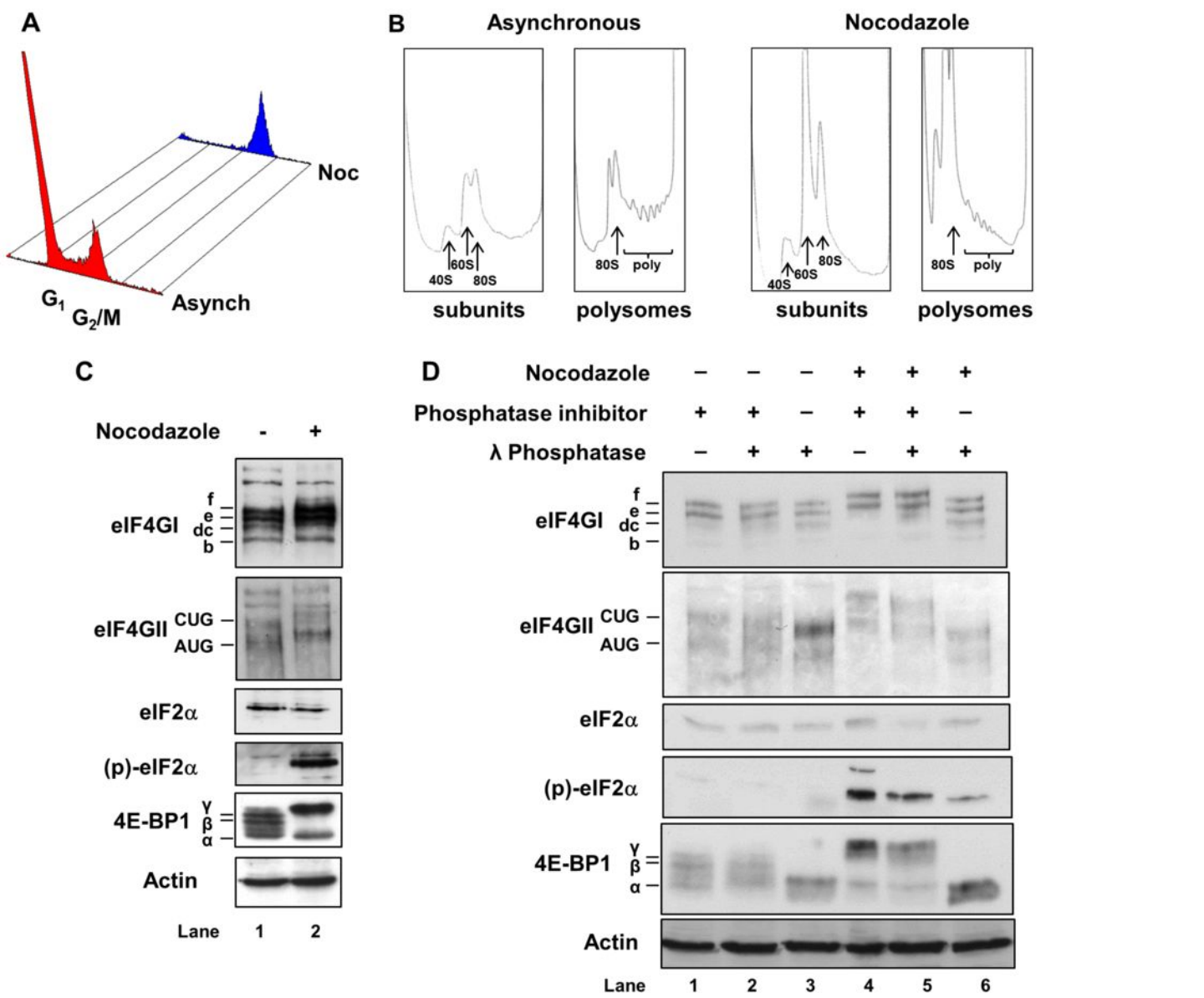
A
Noc
G1
G2/M
Asynch
B
Asynchronous
Nocodazole
40S
60S
80S
80S
poly
40S
60S
80S
80S
poly
subunits
polysomes
subunits
polysomes
C
Nocodazole - +
eIF4GI
f
e
dc
b
eIF4GII
CUG
AUG
eIF2α
(p)-eIF2α
4E-BP1
γ
β
α
Actin
Lane 1 2
D
Nocodazole – – – + + +
Phosphatase inhibitor + + – + + –
λ Phosphatase – + + – + +
eIF4GI
f
e
dc
b
eIF4GII
CUG
AUG
eIF2α
(p)-eIF2α
4E-BP1
γ
β
α
Actin
Lane 1 2 3 4 5 6

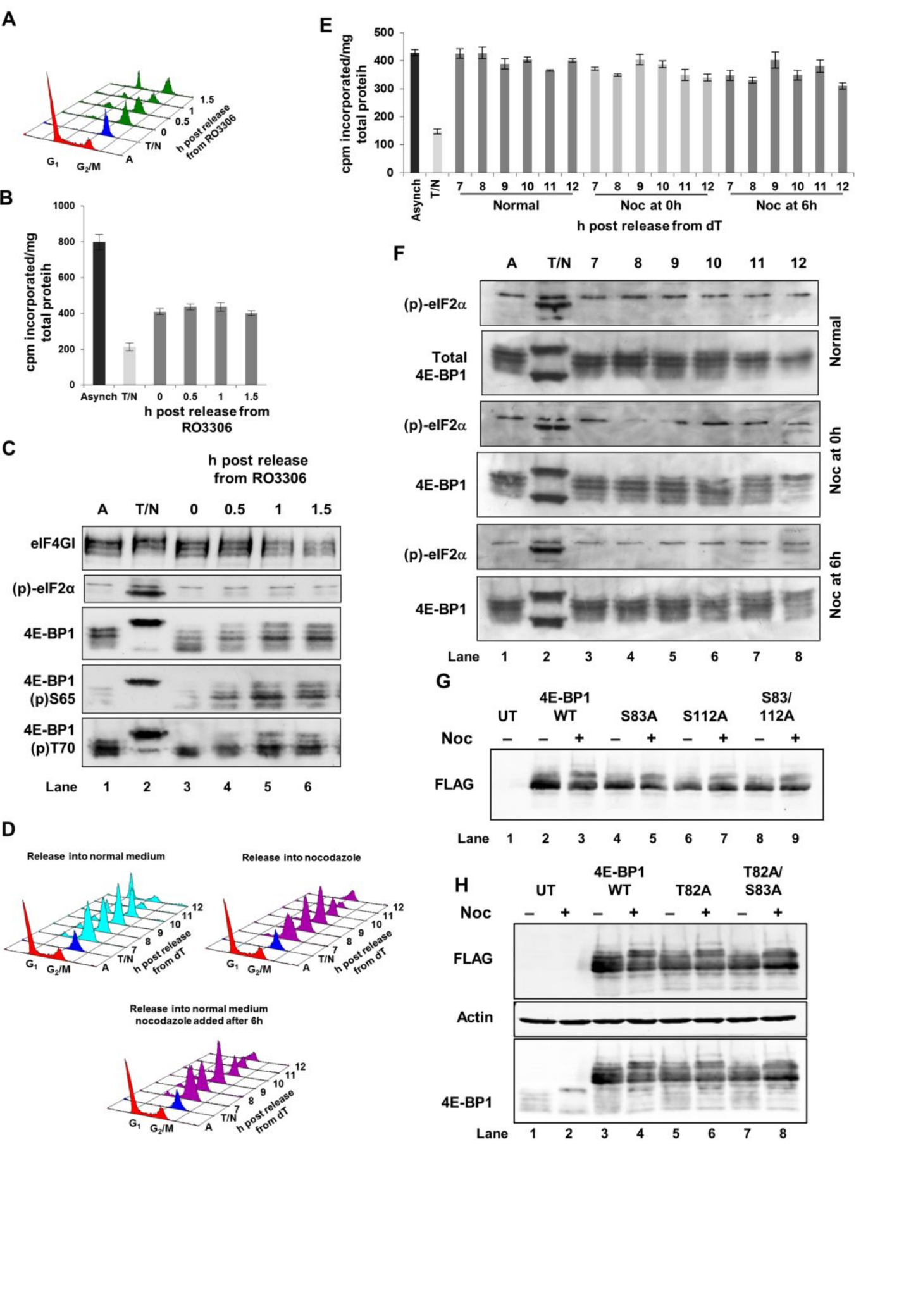
A
G1
G2/M
A
T/N
0
0.5
1
1.5
h post release from RO3306
B
cpm incorporated/mg total proteih
1000
800
600
400
200
0
Asynch
T/N
0
0.5
1
1.5
h post release from RO3306
C
h post release from RO3306
A
T/N
0
0.5
1
1.5
eIF4GI
(p)-eIF2α
4E-BP1
4E-BP1 (p)S65
4E-BP1 (p)T70
Lane 1 2 3 4 5 6
D
Release into normal medium
Release into nocodazole
Release into normal medium nocodazole added after 6h
G1
G2/M
A
T/N
7
8
9
10
11
12
h post release from dT
E
cpm incorporated/mg total proteih
500
400
300
200
100
0
Asynch
T/N
7 8 9 10 11 12
Normal
7 8 9 10 11 12
Noc at 0h
7 8 9 10 11 12
Noc at 6h
h post release from dT
F
A
T/N
7
8
9
10
11
12
(p)-eIF2α
Total 4E-BP1
(p)-eIF2α
4E-BP1
(p)-eIF2α
4E-BP1
Normal
Noc at 0h
Noc at 6h
Lane 1 2 3 4 5 6 7 8
G
UT
4E-BP1 WT
S83A
S112A
S83/ 112A
Noc
– – + – + – + – +
FLAG
Lane 1 2 3 4 5 6 7 8 9
H
UT
4E-BP1 WT
T82A
T82A/ S83A
Noc
– + – + – + – +
FLAG
Actin
4E-BP1
Lane 1 2 3 4 5 6 7 8

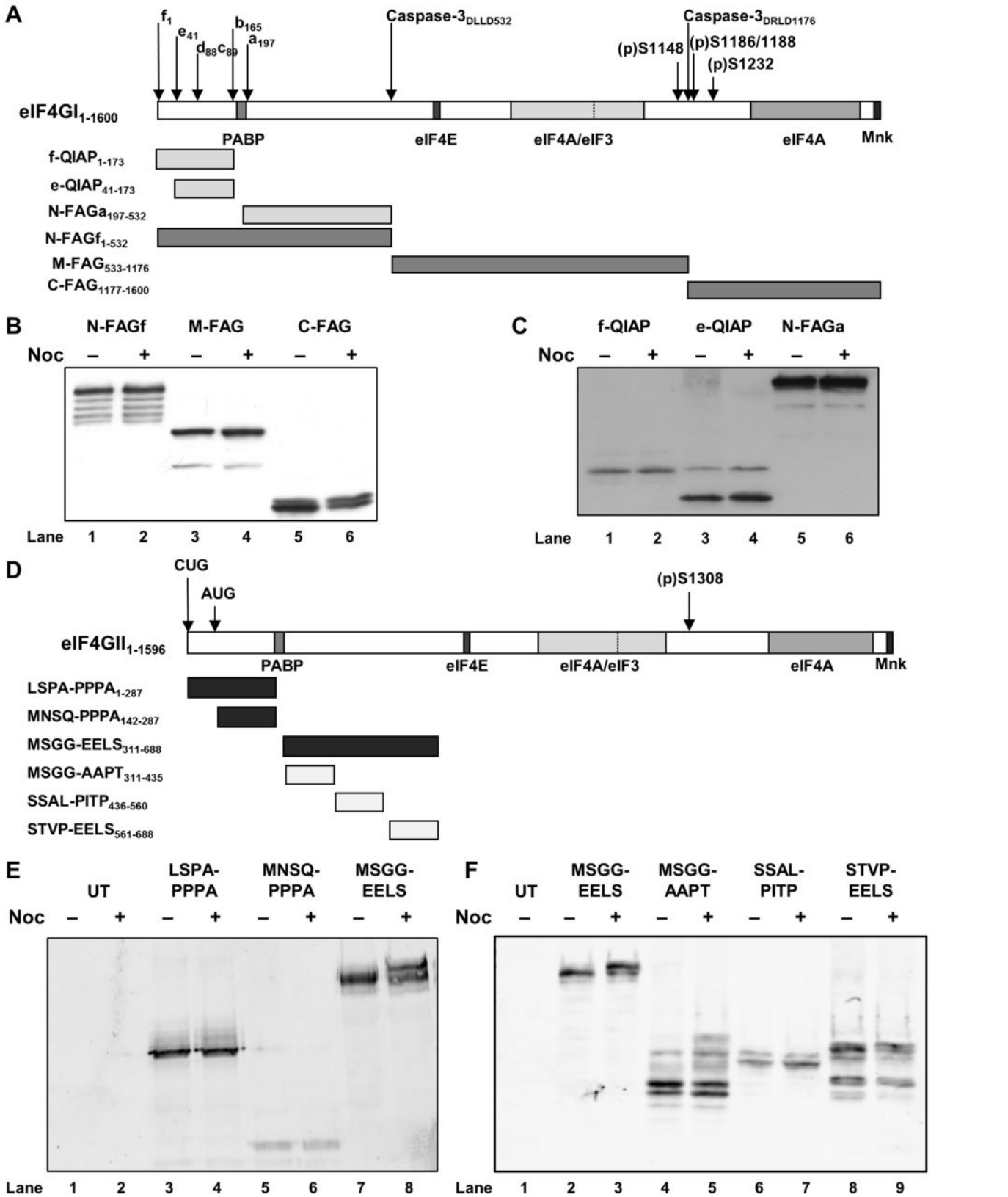
A
f1
e41
d88c89
b165
a197
Caspase-3DLLD532
Caspase-3DRLD1176
(p)S1148
(p)S1186/1188
(p)S1232
eIF4GI1-1600
PABP
eIF4E
eIF4A/eIF3
eIF4A
Mnk
f-QIAP1-173
e-QIAP41-173
N-FAGa197-532
N-FAGf1-532
M-FAG533-1176
C-FAG1177-1600
B
N-FAGf
M-FAG
C-FAG
Noc – + – + – +
Lane 1 2 3 4 5 6
C
f-QIAP
e-QIAP
N-FAGa
Noc – + – + – +
Lane 1 2 3 4 5 6
D
CUG
AUG
(p)S1308
eIF4GII1-1596
PABP
eIF4E
eIF4A/eIF3
eIF4A
Mnk
LSPA-PPPA1-287
MNSQ-PPPA142-287
MSGG-EELS311-688
MSGG-AAPT311-435
SSAL-PITP436-560
STVP-EELS561-688
E
UT
LSPA-PPPA
MNSQ-PPPA
MSGG-EELS
Noc – + – + – + – +
Lane 1 2 3 4 5 6 7 8
F
UT
MSGG-EELS
MSGG-AAPT
SSAL-PITP
STVP-EELS
Noc – – + – + – + – +
Lane 1 2 3 4 5 6 7 8 9

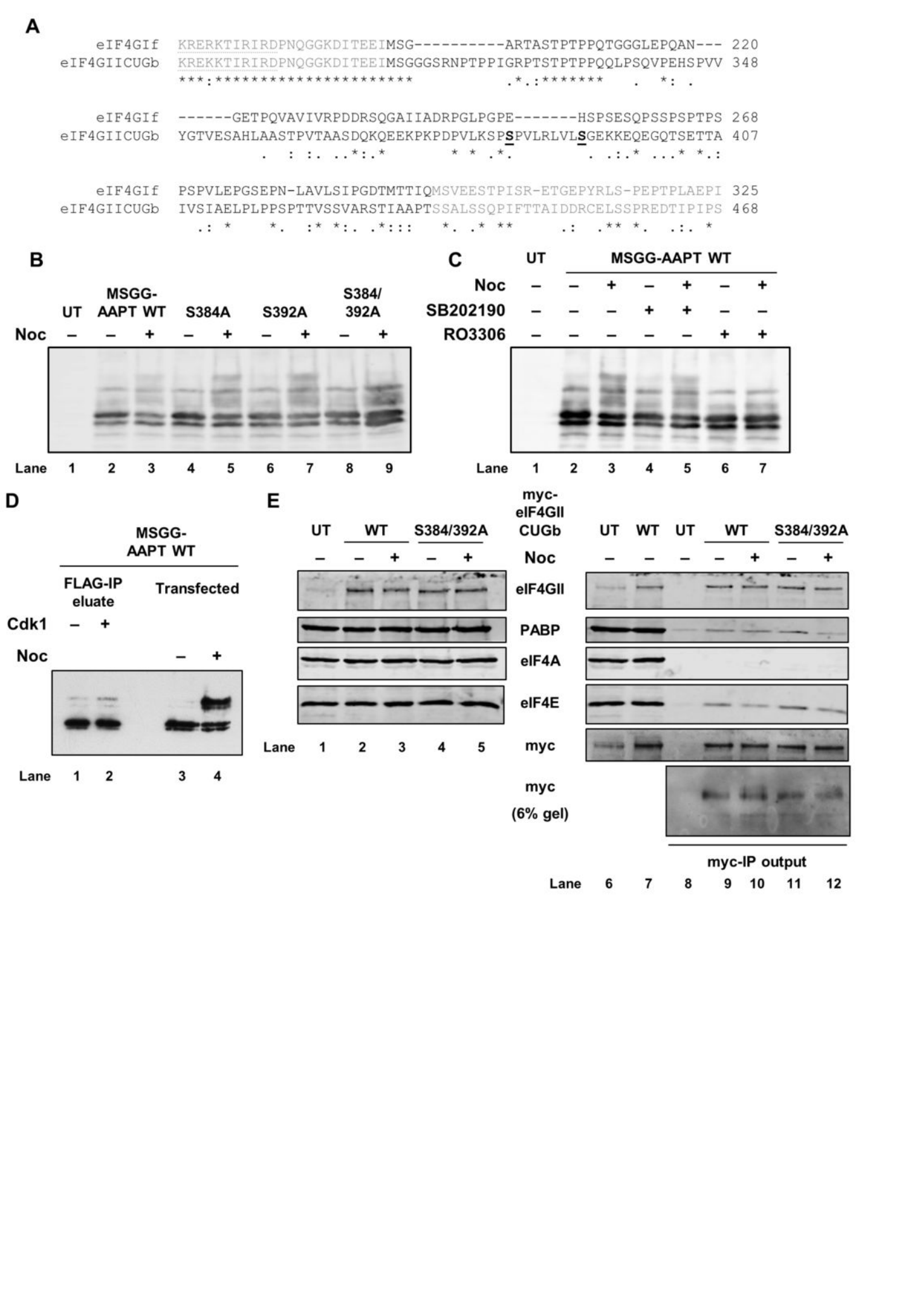
A
eIF4GIf KRERKTIRIRDPNQGGKDITEEIMSG----------ARTASTPTPPQTGGGLEPQAN--- 220
eIF4GIICUGb KREKKTIRIRDPNQGGKDITEEIMSGGGSRNPTPPIGRPTSTPTPPQQLPSQVPEHSPVV 348
eIF4GIf ------GETPQVAVIVRPDDRSQGAIIADRPGLPGPE-------HSPSESQPSSPSPTPS 268
eIF4GIICUGb YGTVESAHLAASTPVTAASDQKQEEKPKPDPVLKSPSPVLRLVLSGEKKEQEGQTSETTA 407
eIF4GIf PSPVLEPGSEPN-LAVLSIPGDTMTTIQMSVEESTPISR-ETGEPYRLS-PEPTPLAEPI 325
eIF4GIICUGb IVSIAELPLPPSPTTVSSVARSTIAAPTSSALSSQPIFTTAIDDRCELSSPREDTIPIPS 468
B
UT
MSGG-AAPT WT
S384A
S392A
S384/392A
Noc
Lane 1 2 3 4 5 6 7 8 9
C
UT
MSGG-AAPT WT
Noc
SB202190
RO3306
Lane 1 2 3 4 5 6 7
D
MSGG-AAPT WT
FLAG-IP eluate
Transfected
Cdk1
Noc
Lane 1 2 3 4
E
UT
WT
S384/392A
Noc
eIF4GII
PABP
eIF4A
eIF4E
myc
Lane 1 2 3 4 5
myc-eIF4GII CUGb
myc (6% gel)
myc-IP output
Lane 6 7 8 9 10 11 12

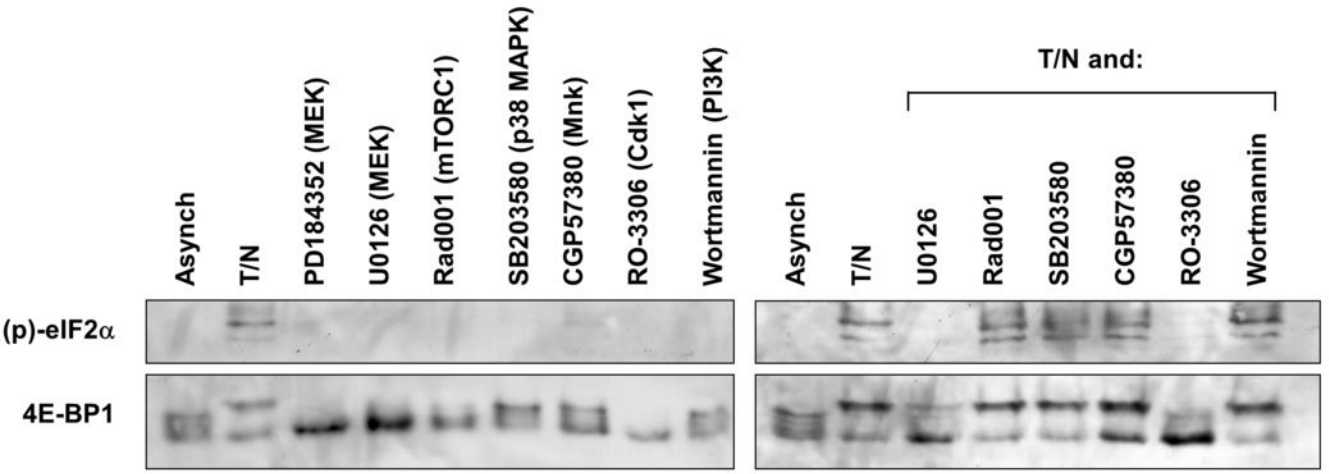
Asynch
T/N
PD184352 (MEK)
U0126 (MEK)
Rad001 (mTORC1)
SB203580 (p38 MAPK)
CGP57380 (Mnk)
RO-3306 (Cdk1)
Wortmannin (PI3K)
T/N and:
Asynch
T/N
U0126
Rad001
SB203580
CGP57380
RO-3306
Wortmannin
(p)-eIF2α
4E-BP1

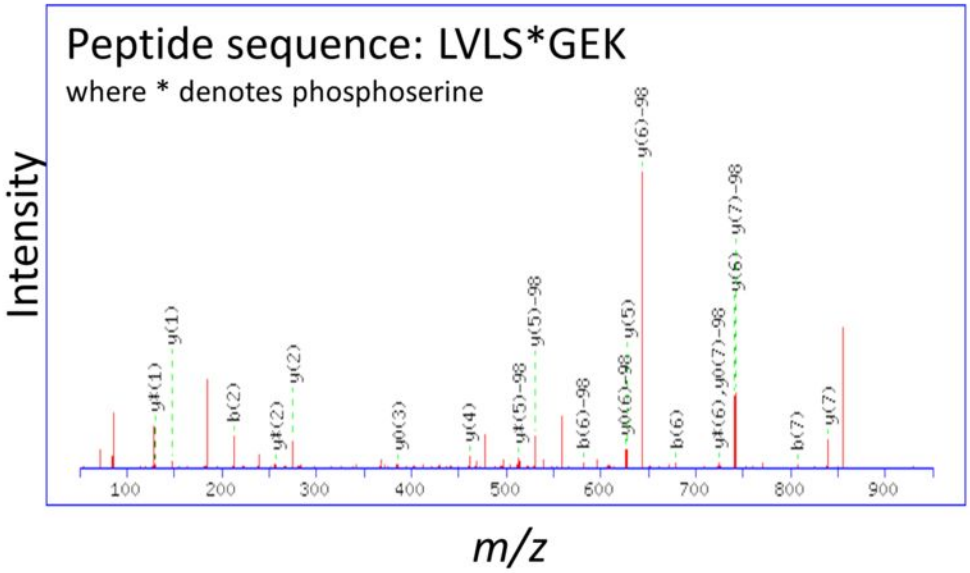
Peptide sequence: LVLS*GEK
where * denotes phosphoserine
Intensity
m/z

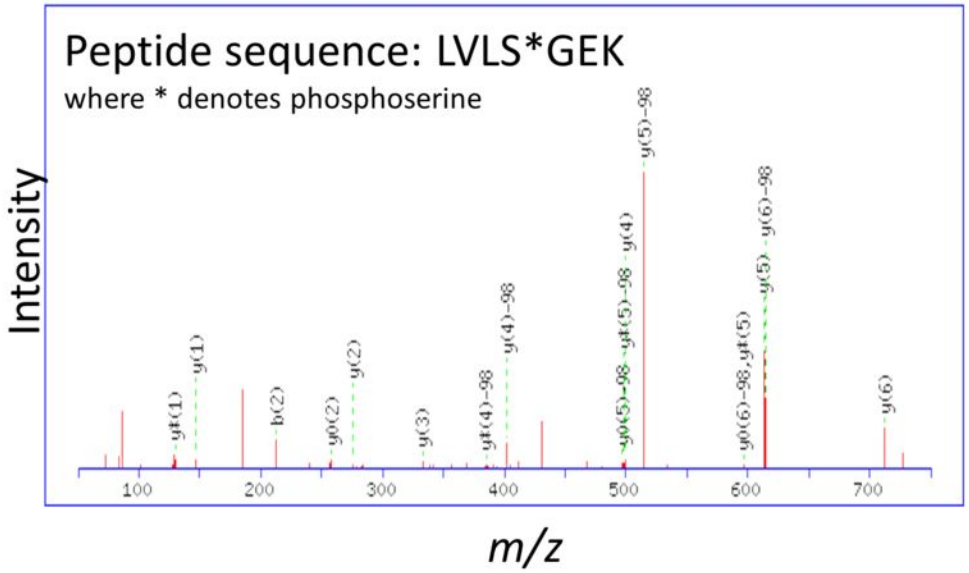
Peptide sequence: LVLS*GEK
where * denotes phosphoserine
Intensity
m/z

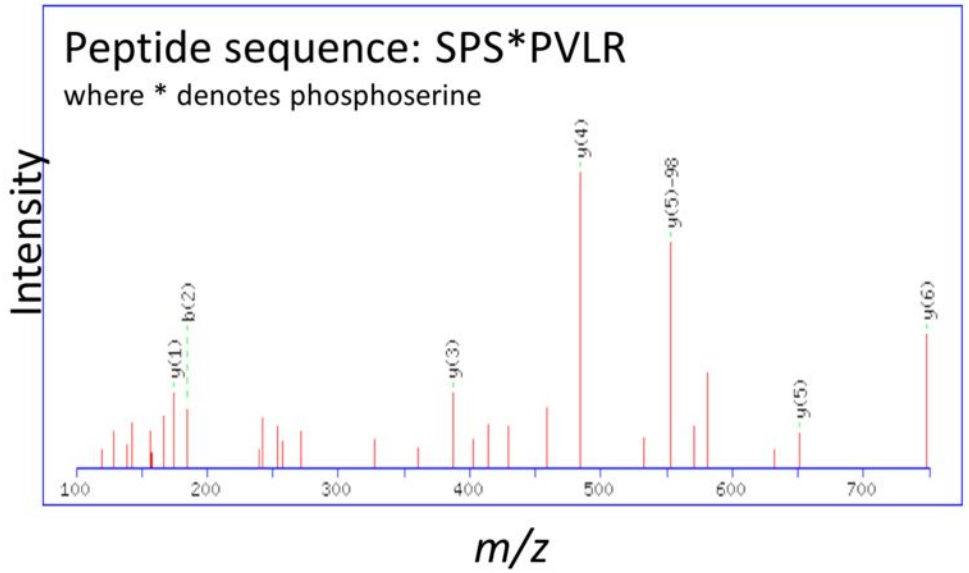
Peptide sequence: SPS*PVLR
where * denotes phosphoserine
Intensity
m/z